

Supporting information for

7-Azaindole breaks carboxylic acid dimers and simplifies VCD spectra analyses of natural products

Corentin Grassin,^[a] Ernesto Santoro^[a] and Christian Merten^{[a],*}

a) Ruhr Universität Bochum
Fakultät für Chemie und Biochemie, Organische Chemie II
Universitätsstraße 150
44801 Bochum, Germany
christian.merten@ruhr-uni-bochum.de
www.mertenlab.de

1.	Experimental and computational details.....	2
2.	Additional spectra.....	3
3.	Computational data.....	6
4.	References	12

1. Experimental and computational details

IR and VCD spectroscopy.

The IR and VCD spectra were recorded on a Bruker Vertex FT-IR spectrometer equipped with a PMA 50 module for VCD measurements. Samples were held in a transmission cell with BaF₂ windows and 100 μm path length. Concentrations are given in the main text. Spectra were recorded at room temperature with 4 cm⁻¹ spectral resolution by accumulating 32 scans for the IR and ~32000 scans (4 hours accumulation time) for VCD. Baseline correction of the VCD spectra was done by subtraction of the spectra of the solvent recorded under identical conditions.

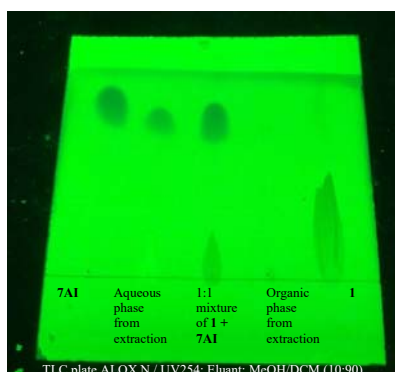
Computational details.

All geometry optimizations and frequency calculations were carried out at B3LYP/6-311++G(2d,p) level of theory using the Gaussian 09 Rev. E software package.¹ Solvent effects were taken into account implicitly by using the integral equation formalism of the polarizable continuum model (IEFPCM)^{2,3} of chloroform. Relative energy differences and Boltzmann populations generally refer to the zero-point corrected energies of the conformers (ΔE_{ZPC}) as we regularly find ΔE_{ZPC} -derived populations to better explain the experimental signatures than Gibbs Free energies (for a detailed discussion see Refs. ⁴⁻⁷, for instance). Vibrational line broadening was simulated by assigning a Lorentzian band shape with half-width at half-height of 6 cm⁻¹ (8 cm⁻¹ for **4** and **4**·**7AI**) to the calculated dipole and rotational strength. The calculated frequencies were scaled by 0.98 to account for anharmonic effects not captured by the harmonic approximation employed in the frequency calculations. Figures were prepared using CYLview.⁸

Recovery of the carboxylic acid

In order to take full advantage of the proposed methodology for AC determinations of valuable samples, the carboxylic acid needs to be recovered, i.e., separated from **7AI**. For **1**·**7AI**, we succeeded by using simple extraction with HCl (1:1 with **7AI** in DCM) followed by another one or two washing steps. The photo below shows a TLC plate which demonstrates that the heterodimer of **1** and **7AI** does not persist on silica and that the two components are easily separable by chromatography. However, note that we did not attempt a quantitative recovery of the carboxylic acids used in this study.

A generally applicable route cannot be given as it depends strongly on the structure of the acid (hydrophilicity, hydrophobicity, ...). The TLC suggests, however, that a separation by chromatographic means is generally feasible and that, for instance, HPLC protocols from the initial natural products separation could also be invoked for the purification of the VCD sample.



2. Additional spectra

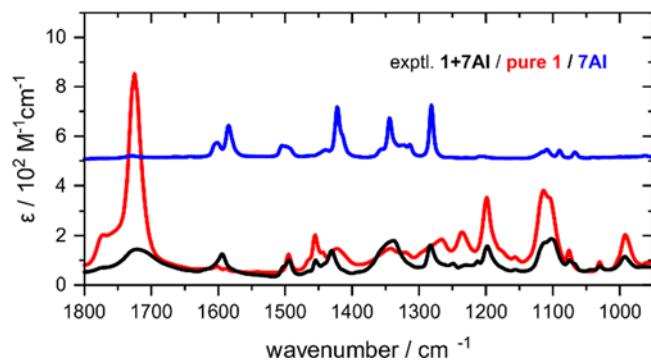


Figure S1. IR spectrum of 7AI compared to the IR spectra of **1** and **1** + 1eq 7AI.

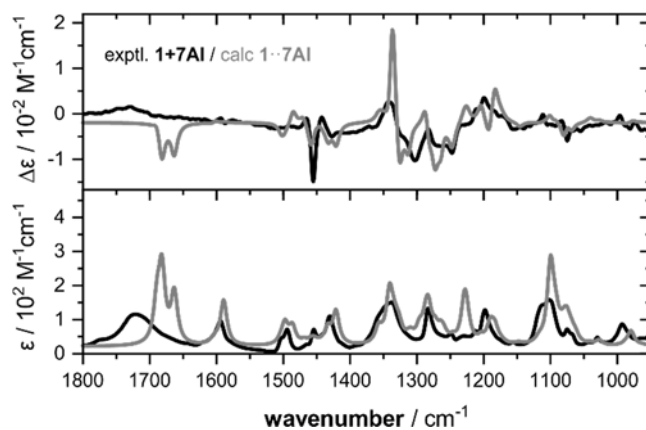


Figure S2. Overlap of the experimental and computed spectra of **1** + 1eq 7AI.

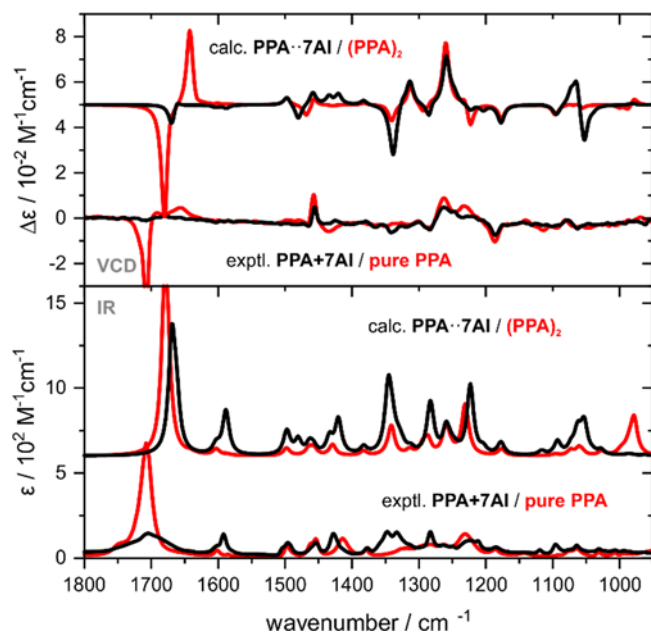


Figure S3. Comparison of the experimental IR and VCD spectra of (R)-2-phenyl propionic acid (PPA) and **PPA** + 1eq **7AI** with the computed spectra of **(PPA)₂** (*J. Phys. Chem. B* 2018, **122**, 8056–8064) and **PPA·7AI** (Tab. S6/S7).

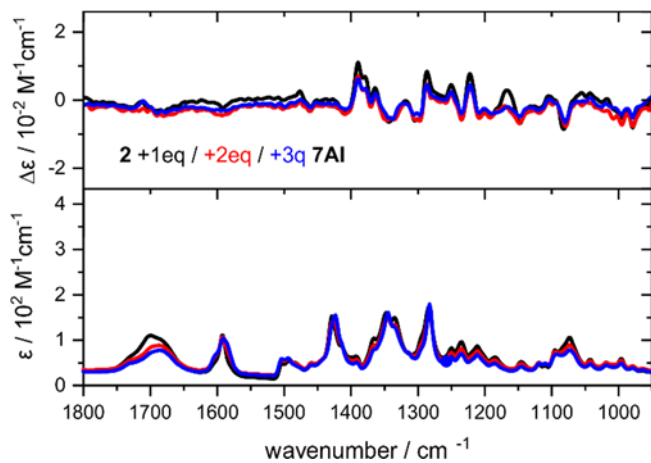


Figure S4. IR and VCD spectra of **2** with different amounts of **7AI**.

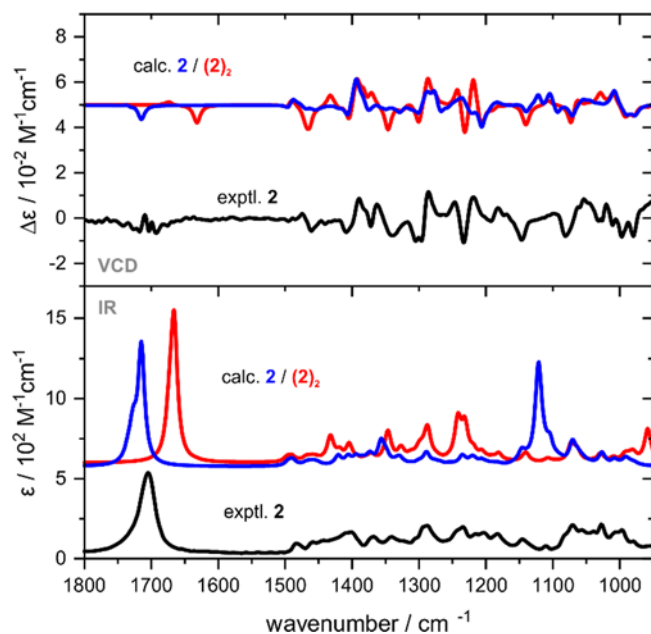


Figure S5. IR and VCD spectra of **2** compared to the computed spectra of monomeric and dimeric **2**.

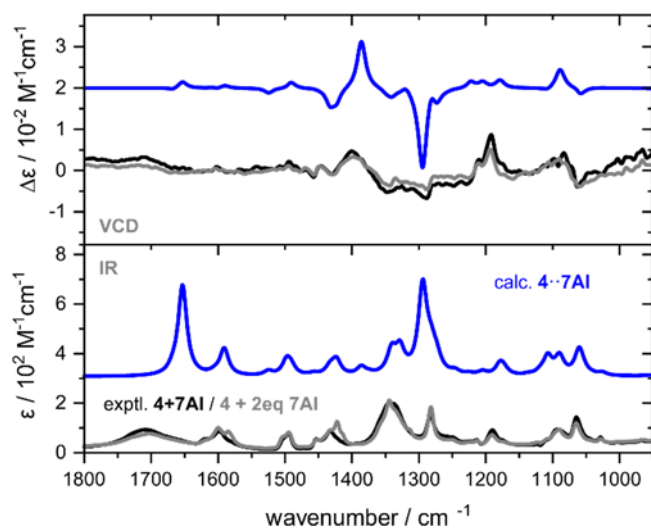


Figure S6. IR and VCD spectra of **4** with 1 and 2 eq of **7AI** compared to the computed spectra of **4·7AI** (cf. Tab. S11). Unlike the other computed spectra, the spectra of **4·7AI** were simulated with 8 cm^{-1} HWHH and the intensities were scaled by 0.5 for better comparison.

3. Computational data



Scheme S1. Torsional angle definitions of (*R*)-**1**.
The COOH moiety is considered in the trans-conformation.

Table S1. Conformers of monomeric (*R*)-**1** as defined by the torsional angles shown in Scheme S1, their relative zero-point corrected and Gibbs free energies (ΔE_{ZPC} and ΔG_{298K} , in kcal/mol) and the corresponding Boltzmann weights χ (in percentage).

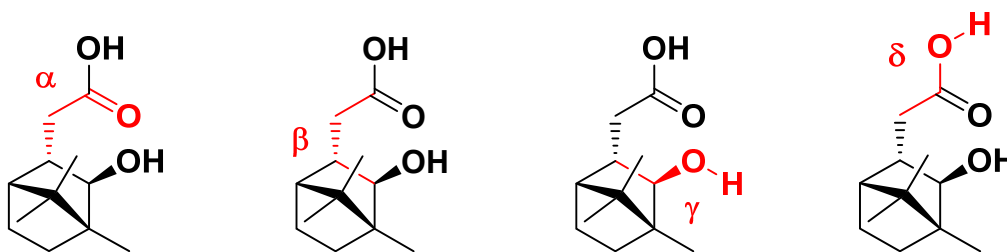
	α / deg	β / deg	ΔE_{ZPC}	ΔG_{298K}	$\chi(\Delta E_{ZPC})$	$\chi(\Delta G_{298K})$
1-c1	-21.9	-71.6	0.0 ^{a)}	0.0 ^{b)}	44.0	45.7
1-c2	-23.3	-167.2	0.39	0.45	22.9	21.2
1-c3	148.7	-69.5	0.44	0.45	20.8	21.3
1-c4	146.8	-164.9	0.79	0.83	11.6	11.4
1-c5	-16.4	78.1	2.59	2.90	0.6	0.3
1-c6	178.3	78.0	3.58	3.63	0.1	0.1

^{a)} referenced to $E_{ZPC}(\mathbf{c1}) = -574.661329$ hartree. ^{b)} referenced to $G(\mathbf{c1}) = -574.699929$ hartree.

Table S2. Conformers of (*R*)-**1**-**7AI**, their relative zero-point corrected and Gibbs free energies (ΔE_{ZPC} and ΔG_{298K} , in kcal/mol) and the corresponding Boltzmann weights χ (in percentage).

	α / deg	β / deg	ΔE_{ZPC}	ΔG_{298K}	$\chi(\Delta E_{ZPC})$	$\chi(\Delta G_{298K})$
1-7AI -c1	-24.2	-71.0	0.0 ^{a)}	0.0 ^{b)}	44.9	67.0
1-7AI -c2	-24.5	-166.4	0.40	0.83	22.7	16.4
1-7AI -c3	150.5	-69.3	0.43	1.10	21.6	10.6
1-7AI -c4	148.0	-165.1	0.87	1.46	10.3	5.7
1-7AI -c5	-15.2	78.4	2.77	3.45	0.4	0.2
1-7AI -c6	169.2	79.9	3.47	3.99	0.1	0.1

^{a)} referenced to $E_{ZPC}(\mathbf{c1}) = -954.539472$ hartree. ^{b)} referenced to $G(\mathbf{c1}) = -954.59127$ hartree.



Scheme S2. Torsional angle definitions of (*1R*)-**2**.

Table S3. Conformers of monomeric (*1R*)-**2** as defined by the torsional angles shown in Scheme S2, their relative zero-point corrected and Gibbs free energies (ΔE_{ZPC} and ΔG_{298K} , in kcal/mol) and the corresponding Boltzmann weights χ (in percentage).

	α / deg	β / deg	γ / deg	δ / deg	ΔE_{ZPC}	ΔG_{298K}	$\chi(\Delta E_{ZPC})$	$\chi(\Delta G_{298K})$
2-c1	9.3	-66.3	-56.1	-178.7	0.0a)	0.0b)	76.74	58.81
2-c2	-161.9	-71.9	-169.0	-0.3	1.45	1.86	6.65	2.52
2-c3	-121.6	-179.3	-169.6	-179.9	1.75	0.96	4.00	11.70
2-c4	105.5	-65.2	-166.4	177.6	1.81	1.30	3.60	6.53
2-c5	-77.6	-70.9	-169.2	-177.8	2.08	1.49	2.28	4.76
2-c6	-132.2	-77.8	-66.1	178.9	2.15	1.77	2.02	2.95
2-c7	23.2	-173.3	-74.3	-177.4	2.31	1.46	1.55	4.97
2-c8	20.8	-172.6	60.2	-177.3	2.46	1.69	1.22	3.36
2-c9	-118.2	-179.7	-77.3	-179.5	2.58	1.77	0.99	2.94
2-c10	8.6	-66.3	-56.0	1.3	3.04	3.11	0.45	0.31
2-c11	-121.0	-179.4	61.7	-180.0	3.06	2.39	0.44	1.05
2-c12	-58.1	54.4	-166.4	177.1	4.79	4.59	0.02	0.03
2-c13	-117.7	-179.3	-169.2	0.7	4.88	4.53	0.02	0.03
2-c14	108.9	-62.9	-164.5	0.4	5.13	4.51	0.01	0.03
2-c15	117.7	63.7	-167.8	-178.3	5.34	5.26	0.01	0.01

^{a)} referenced to $E_{ZPC}(\mathbf{c1}) = -694.924515$ hartree. ^{b)} referenced to $G(\mathbf{c1}) = -694.965251$ hartree.

Table S4. Conformers of dimeric [(*IR*)-2]₂, their relative zero-point corrected and Gibbs free energies (ΔE_{ZPC} and ΔG_{298K} , in kcal/mol) and the corresponding Boltzmann weights χ (in percentage).

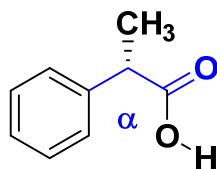
	α / deg	β / deg	γ / deg	α / deg	β / deg	γ / deg	ΔE_{ZPC}	ΔG_{298K}	$\chi(\Delta E_{ZPC})$	$\chi(\Delta G_{298K})$
2-c1-c1	7.8	-67.1	-55.6	7.8	-67.1	-55.6	0.00	0.00	64.45	32.84
2-c1-c3	10.1	-67.7	-55.8	-120.9	-178.8	-169.7	1.22	0.53	8.25	13.51
2-c1-c4	8.4	-67.1	-55.4	103.4	-67.0	-167.8	1.26	0.53	7.68	13.33
2-c1-c5	10.7	-67.5	-55.9	-178.4	-77.3	-68.4	1.32	0.68	6.99	10.42
2-c1-c6	11.4	-68.4	-55.8	-143.2	-76.6	-63.6	1.39	0.64	6.15	11.13
2-c3-c3	-120.8	-178.9	-169.9	-120.8	-178.9	-169.9	2.65	1.37	0.73	3.26
2-c3-c4	-122.1	-178.7	-169.9	104.9	-66.0	-167.0	2.67	1.56	0.71	2.37
2-c3-c5	-124.0	-179.0	-170.1	-77.0	-69.6	-168.1	2.84	1.66	0.53	2.01
2-c3-c6	-124.3	-178.0	-169.8	-151.1	-75.3	-61.6	2.56	1.37	0.86	3.27
2-c4-c4	104.7	-65.7	-164.3	104.7	-65.7	-164.3	2.71	1.62	0.66	2.13
2-c4-c5	104.4	-67.2	-167.6	-76.2	-69.5	-167.9	2.88	1.85	0.50	1.43
2-c4-c6	102.3	-66.8	-168.0	-151.5	-75.4	-61.0	2.64	1.94	0.75	1.25
2-c5-c5	-75.4	-68.7	-165.2	-75.4	-68.7	-165.2	2.93	1.89	0.46	1.36
2-c5-c6	-76.9	-69.6	-168.3	-151.2	-75.2	-61.1	2.76	2.14	0.61	0.89
2-c6-c6	-149.1	-75.9	-62.0	-149.1	-75.9	-62.0	2.70	2.20	0.67	0.80

^{a)} referenced to $E_{ZPC}(\mathbf{c1}) = -1389.865499$ hartree. ^{b)} referenced to $G(\mathbf{c1}) = -1389.928613$ hartree.

Table S5. Conformers of monomeric (*IR*)-2·7Al, their relative zero-point corrected and Gibbs free energies (ΔE_{ZPC} and ΔG_{298K} , in kcal/mol) and the corresponding Boltzmann weights χ (in percentage).

	α / deg	β / deg	γ / deg	ΔE_{ZPC}	ΔG_{298K}	$\chi(\Delta E_{ZPC})$	$\chi(\Delta G_{298K})$
2-c1	9.6	-67.3	-54.4	0.0 ^{a)}	0.0 ^{b)}	83.3	61.8
2-c2	n/a						
2-c3	-125.4	-178.7	-169.2	1.94	1.01	3.1	11.2
2-c4	104.6	-67.2	-166.8	2.20	1.55	2.0	4.5
2-c5	-73.3	-70.2	-167.3	2.27	1.54	1.8	4.6
2-c6	-153.2	-74.8	-58.9	1.48	1.03	6.8	10.9
2-c7	31.0	-173.4	-72.2	2.50	1.81	1.3	2.9
2-c8	24.3	-172.2	58.9	2.74	2.15	0.8	1.6
2-c9	-120.9	-178.7	-74.1	2.71	1.91	0.9	2.5

^{a)} referenced to $E_{ZPC}(\mathbf{c1}) = -1074.801672$ hartree. ^{b)} referenced to $G(\mathbf{c1}) = -1074.854694$ hartree.



Scheme S3. Torsional angle definitions of **2-phenyl propionic acid (PPA)**.
The COOH moiety is considered in the trans-conformation.

Table S6. Conformers of monomeric (*S*)-**PPA** as defined by the torsional angles shown in Scheme S3, their relative zero-point corrected and Gibbs free energies (ΔE_{ZPC} and ΔG_{298K} , in kcal/mol) and the corresponding Boltzmann weights χ (in percentage).

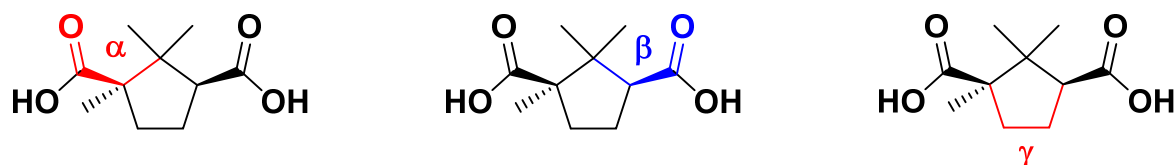
	α	ΔE_{ZPC}	ΔG_{298K}	$\chi(\Delta E_{ZPC})$	$\chi(\Delta G_{298K})$
PPA-c1	-96.9	0.0 ^{a)}	0.0 ^{b)}	80.7	78.6
PPA-c2	97.5	0.85	0.77	19.3	21.4

^{a)} referenced to $E_{ZPC}(\mathbf{c1}) = -499.440249$ hartree. ^{b)} referenced to $G(\mathbf{c1}) = -499.477101$ hartree.

Table S7. Conformers of (*S*)-**PPA**·**7AI**, their relative zero-point corrected and Gibbs free energies (ΔE_{ZPC} and ΔG_{298K} , in kcal/mol) and the corresponding Boltzmann weights χ (in percentage).

	α	ΔE_{ZPC}	ΔG_{298K}	$\chi(\Delta E_{ZPC})$	$\chi(\Delta G_{298K})$
PPA·7AI-c1	-94.7	0.0 ^{a)}	0.0 ^{b)}	73.7	80.4
PPA·7AI-c2	95.3	0.61	0.84	26.3	19.6

^{a)} referenced to $E_{ZPC}(\mathbf{c1}) = -879.317294$ hartree. ^{b)} referenced to $G(\mathbf{c1}) = -879.367061$ hartree.



Scheme S4. Torsional angle definitions of **3**.
The COOH moiety is considered in the trans-conformation.

Table S8. Conformers of monomeric **3** as defined by the torsional angles shown in Scheme S4, their relative zero-point corrected and Gibbs free energies (ΔE_{ZPC} and ΔG_{298K} , in kcal/mol) and the corresponding Boltzmann weights χ (in percentage).

	α / deg	β / deg	γ / deg	ΔE_{ZPC}	ΔG_{298K}	$\chi(\Delta E_{ZPC})$	$\chi(\Delta G_{298K})$
3-c1	-112.2	98.4	11.2	0.0 ^{a)}	0.0 ^{b)}	54.2	51.7
3-c2	71.5	100.6	16.6	0.50	0.43	23.3	25.2
3-c3	-112.0	-83.9	1.3	1.03	1.05	9.4	8.8
3-c4	-111.7	-14.3	1.3	1.22	1.25	6.9	6.3
3-c5	71.0	-82.8	14.3	1.52	1.29	4.2	5.9
3-c6	72.3	-17.9	6.4	1.95	1.88	2.0	2.1

^{a)} referenced to $E_{ZPC}(\mathbf{c1}) = -691.612329$ hartree. ^{b)} referenced to $G(\mathbf{c1}) = -691.653728$ hartree.

Table S9. Conformers of **7AI·3·7AI**, their relative zero-point corrected and Gibbs free energies (ΔE_{ZPC} and ΔG_{298K} , in kcal/mol) and the corresponding Boltzmann weights χ (in percentage).

	α / deg	β / deg	γ / deg	ΔE_{ZPC}	ΔG_{298K}	$\chi(\Delta E_{ZPC})$	$\chi(\Delta G_{298K})$
7AI·3·7AI-c1	-111.2	98.3	11.1	0.0 ^{a)}	0.0 ^{b)}	50.9	59.8
7AI·3·7AI-c2	70.4	99.8	16.0	0.48	0.65	22.8	20.0
7AI·3·7AI-c3	-111.9	-83.7	9.4	0.78	1.05	13.6	10.1
7AI·3·7AI-c4	-111.0	-21.9	3.9	1.44	1.66	4.5	3.6
7AI·3·7AI-c5	69.8	-82.2	14.7	1.24	1.52	6.2	4.6
7AI·3·7AI-c6	71.8	-27.7	8.3	1.92	2.03	2.0	1.9

^{a)} referenced to $E_{ZPC}(\mathbf{c1}) = -1451.366086$ hartree. ^{b)} referenced to $G(\mathbf{c1}) = -1451.432812$ hartree.

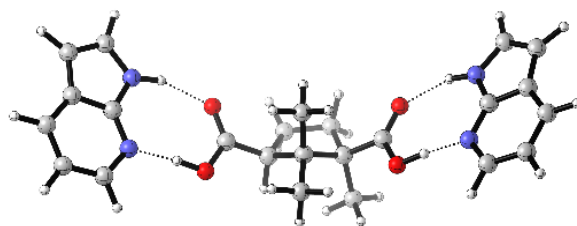
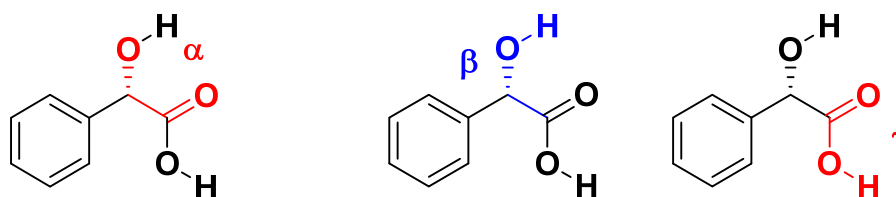


Figure S7. Structure of the lowest energy conformer **7AI·3·7AI-c1**.



Scheme S5. Torsional angle definitions of **4**.

Table S10. Conformers of monomeric (*S*)-**4** as defined by the torsional angles shown in Scheme S5, their relative zero-point corrected and Gibbs free energies (ΔE_{ZPC} and ΔG_{298K} , in kcal/mol) and the corresponding Boltzmann weights χ (in percentage).

	α / deg	β / deg	γ / deg	ΔE_{ZPC}	ΔG_{298K}	$\chi(\Delta E_{ZPC})$	$\chi(\Delta G_{298K})$
4-c1	-7.4	4.1	-1.2	0.0 ^{a)}	0.0 ^{b)}	78.6	77.0
4-c2	168.9	151.9	-177.3	0.98	0.89	15.0	17.0
4-c3	-22.1	174.3	-2.5	2.13	2.20	2.2	1.9
4-c4	10.8	-12.7	-174.0	2.21	2.69	1.9	0.8
4-c5	147.6	64.3	0.5	2.44	2.36	1.3	1.4
4-c6	164.8	-47.8	0.5	2.56	2.18	1.0	1.9

^{a)} referenced to $E_{ZPC}(\mathbf{c1}) = -535.382145$ hartree. ^{b)} referenced to $G(\mathbf{c1}) = -535.418706$ hartree.

Table S11. Conformers of (*S*)-**4**·**7AI**, their relative zero-point corrected and Gibbs free energies (ΔE_{ZPC} and ΔG_{298K} , in kcal/mol) and the corresponding Boltzmann weights χ (in percentage).

	α / deg	β / deg	ΔE_{ZPC}	ΔG_{298K}	$\chi(\Delta E_{ZPC})$	$\chi(\Delta G_{298K})$
4·7AI-c1	-7.6	4.4	0.0	0.0	94.0	91.5
4·7AI-c2	n/a					
4·7AI-c3	-21.6	175.2	2.87	2.60	0.7	1.1
4·7AI-c4	n/a					
4·7AI-c5	n/a					
4·7AI-c6	159.3	20.6 ^{c)}	1.70	1.49	5.3	7.4

^{a)} referenced to $E_{ZPC}(\mathbf{c1}) = -915.261443$ hartree. ^{b)} referenced to $G(\mathbf{c1}) = -915.309966$ hartree.

^{c)} When **7AI**, the heterodimers of both **c5** and **c6** converge to an identical structure, in which β is an intermediate angle between both monomeric structures

4. References

1. *Gaussian 09, Rev E.01*, M. J. Frisch, G. W. Trucks, H. B. Schlegel, G. E. Scuseria, M. A. Robb, J. R. Cheeseman, G. Scalmani, V. Barone, B. Mennucci, G. A. Petersson, H. Nakatsuji, M. Caricato, X. Li, H. P. Hratchian, A. F. Izmaylov, J. Bloino, G. Zheng, J. L. Sonnenberg, M. Hada, M. Ehara, K. Toyota, R. Fukuda, J. Hasegawa, M. Ishida, T. Nakajima, Y. Honda, O. Kitao, H. Nakai, T. Vreven, J. J. A. Montgomery, J. E. Peralta, F. Ogliaro, M. Bearpark, J. J. Heyd, E. Brothers, K. N. Kudin, V. N. Staroverov, T. Keith, R. Kobayashi, J. Normand, K. Raghavachari, A. Rendell, J. C. Burant, S. S. Iyengar, J. Tomasi, M. Cossi, N. Rega, J. M. Millam, M. Klene, J. E. Knox, J. B. Cross, V. Bakken, C. Adamo, J. Jaramillo, R. Gomperts, R. E. Stratmann, O. Yazyev, A. J. Austin, R. Cammi, C. Pomelli, J. W. Ochterski, R. L. Martin, K. Morokuma, V. G. Zakrzewski, G. A. Voth, P. Salvador, J. J. Dannenberg, S. Dapprich, A. D. Daniels, O. Farkas, J. B. Foresman, J. V. Ortiz, J. Cioslowski and D. J. Fox, Wallingford CT, USA, 2013
2. B. Mennucci, C. Cappelli, R. Cammi and J. Tomasi, *Chirality*, 2011, **23**, 717-729.
3. J. Tomasi, B. Mennucci and R. Cammi, *Chem. Rev.*, 2005, **105**, 2999-3094.
4. K. Scholten and C. Merten, *Phys. Chem. Chem. Phys.*, 2022, **24**, 3611-3617.
5. K. Scholten and C. Merten, *Phys. Chem. Chem. Phys.*, 2022, **24**, 4042-4050.
6. M. Kemper, E. Engelage and C. Merten, *Angew. Chem. Int. Ed.*, 2021, **60**, 2958-2962.
7. K. Bünnemann and C. Merten, *Phys. Chem. Chem. Phys.*, 2017, **19**, 18948-18956.
8. *CYLview 1.0b*, C. Y. Legault, Université de Sherbrooke, 2009